# NONLINEARITIES IN SINGLE-CRYSTAL SILICON MICROMECHANICAL RESONATORS

Ville Kaajakari[1,2],Tomi Mattila[1], Jyrki Kiihamäki[1], Hannu Kattelus[1], Aarne Oja[1], and Heikki Seppä[1]
[1]VTT Information Technology, P.O. BOX 1207, 02044 Espoo, Finland
[2]Helsinki University of Technology, Metrology Research Institute,
P.O. BOX 3000, 02015 Espoo, Finland

## ABSTRACT

The fundamental performance limit of single-crystal silicon resonators set by device nonlinearities is characterized. Using Leeson's model for near carrier phase noise, the nonlinearity is shown to set the scaling limit in miniaturizing oscillators. A circuit model based on discretization of distributed mass and nonlinear elasticity is introduced to accurately simulate the large amplitude vibrations. Based on published data for the third-order silicon stiffness tensor, the fundamental material nonlinearity limit is estimated. This theoretical limit is compared to measured nonlinearities in bulk acoustic wave (BAW) micromechanical resonators. The material set and measured nonlinearities are of same order-of-magnitude showing that the maximum vibration amplitude of studied BAW microresonators is near the fundamental limit. The maximum strain for single-crystal silicon resonators set by hysteresis limit is estimated to be $2 \cdot 10^{-3}$ (fracture limit $10^{-2}$), which corresponds to the maximum energy density of $E_m/V = 3 \cdot 10^5$ J/m$^3$. This value is at least two orders-of-magnitude higher than for shear-mode quartz resonators, which partially compensates for the small size of MEMS components.

**Keywords:** nonlinear, phase noise, resonator, RF-MEMS

## I. INTRODUCTION

Fast market growth for portable communication devices has lead to a wide interest in oscillators having small size and low power consumption. Mechanical quartz resonators provide exceptionally high precision and stability. However, the macroscopic size and low integratibility with IC electronics are the major drawbacks of quartz crystals. Micromechanical silicon resonators are an interesting alternative due to their compact size and feasibility of integration with IC technologies. Unfortunately, the small size of MEMS resonators also results in lower energy storage capacity. Therefore the microresonators have to be driven close to the nonlinearity limit for sufficient performance as demonstrated by our 12 MHz bulk acoustic wave (BAW) oscillator ($Q = 180\,000$) [1]. This is in contrast with quartz resonators that due to their large size can more easily provide sufficient signal-to-noise ratio without being driven close to the nonlinear limit.

For BAW resonators both the mechanical and capacitive nonlinearities can be significant. While the capacitive and geometrical nonlinearities are well-understood [1, 2], little information exists about the material induced mechanical nonlinearity in MEMS resonators. Although the silicon material nonlinearity is small and can be ignored in many MEMS applications, it becomes important in determining the maximum vibration amplitude of high quality factor BAW resonators.

In this paper, the effect of mechanical nonlinearity in distributed mass and elasticity is accurately modeled with a chain of discrete elements. The nonlinearity is introduced as first- and second-order displacement dependent corrections to the spring constant following from the large deformation theory of anisotropic solids. The analysis of measured resonator transmission curves shows that the maximum energy density for the studied BAW devices is close to the intrinsic material limit.

## II. NONLINEARITY AND PHASE NOISE IN MICRO-OSCILLATORS

To show the importance of nonlinearities in microresonators, it is useful to consider phase noise in an ideal oscillator. Leeson's model gives the phase noise-to-carrier ratio for a small offset $\Delta\omega$ from the carrier frequency $\omega_0$ as

$$L(\Delta\omega) = 10 \cdot \log\left[\frac{2kT}{E_{stored}}\frac{Q}{\omega_0}\left(1+\left(\frac{\omega_0}{2Q\Delta\omega}\right)^2\right)\right], \quad (1)$$

where $Q$ is the resonator quality factor and $E_{stored}$ is the energy stored in the resonator tank [3, 4]. The first term in the brackets in Equation (1) gives the noise floor and second term gives the near carrier noise. To decrease the near carrier noise, either the tank energy or the quality factor can be increased. However, for a good noise floor the tank energy should be increased but the quality factor decreased. Thus a high quality factor alone does not enable good oscillator and to obtain good overall phase noise, the vibration energy should be maximized.

The amount of energy that can be stored in a microresonator is limited by device nonlinearities. The maximum vibration energy is

$$E_{stored}^{max} = \frac{1}{2}kX_C^2, \quad (2)$$

where $k$ is the mechanical spring constant and $X_C$ is the critical vibration amplitude at the hysteresis limit set by mechanical nonlinearity. These scale as

$$\begin{aligned} k &\sim l \\ X_C &\sim l/\sqrt{\alpha Q}, \end{aligned} \quad (3)$$

where $l$ is the characteristic device dimension and $\alpha$ is the geometry and material dependent nonlinearity constant [5]. Thus at the nonlinearity limit, the maximum vibration energy is $E_{stored}^{max} \sim l^3/\alpha Q$ and the phase noise-to-carrier spectrum is

$$L(\Delta\omega) \sim \frac{\alpha}{l^3}\left(\frac{Q^2}{\omega_0}+\frac{\omega_0}{4\Delta\omega^2}\right). \quad (4)$$

Equation (4) indicates that if the power output of the oscillator is limited by the device nonlinearities, the near carrier noise



0-7803-7731-1/03/$17.00 ©2003 IEEE

***Table 1.*** *Calculated values for the nonlinear engineering Young's modulus*

| | $Y_0$[GPa] | $Y_1$ | $Y_2$ |
|---|---|---|---|
| 1–D Beam ([100]) | 130 | 0.65 | -4.6 |
| 2–D Plate | 181 | -2.8 | -8.3 |

does not depend on the quality factor and the noise floor degrades as a square of the tank quality factor. Thus, the device nonlinearities set the fundamental scaling limit for microresonators and the small size cannot be compensated with a high quality factor. Macroscale resonators do not suffer from this problem as they are large enough to store sufficient energy without being driven to the nonlinear limit.

## III. Mechanical Nonlinearity in Silicon BAW Resonators

Large amplitude vibrations can lead to two types of anharmonic effects of mechanical origin: geometrical and material nonlinearity. Geometrical effects have been studied in flexural resonators. For example clamped-clamped beams demonstrate increasing tension with displacement leading to spring hardening in the restorative force [2]. For bulk acoustic wave resonators, however, the geometrical nonlinearity is not dominant and material effects have to be included. To include these nonlinearities large deformation theory has to be used. The Cauchy stress due to finite deformation including both the geometrical (area and volume change) and material stiffness effects is

$$\sigma_{ij}(X) = \frac{\rho_X}{\rho_a}\frac{\partial X_i}{\partial a_k}\frac{\partial X_j}{\partial a_k}(c_{ijkl}\eta_{kl} + c_{ijklmn}\eta_{kl}\eta_{mn}), \qquad (5)$$

where $X$ is the particle coordinate at finite deformation, $a$ is the undeformed state, $\rho_X$ and $\rho_a$ are the deformed and undeformed densities, $c_{ijk}$ and $c_{ijlmn}$ are the second and third order stiffness tensors, and $\eta_{kl}$ is the Lagrangian strain [6]. The third-order stiffness tensor has been measured using ultrasonic wave measurements [7]. This data and Equation (5) enable computation of nonlinear strain dependent engineering Young's modulus

$$Y = \frac{T}{S} = Y_0(1 + Y_1 S + Y_2 S^2), \qquad (6)$$

where $T$ is the force divided by the initial undeformed area (engineering stress), $S = \partial u/\partial x$ is the displacement gradient with respect undeformed coordinates (engineering strain), and $Y_1$ and $Y_2$ are the first- and second-order corrections respectively.

Calculated values for nonlinear Young's modulus are tabulated in Table 1 with values in [100]-direction agreeing with published analytical results in reference [6]. Unfortunately, no information exist on the effect of doping on the anharmonic stiffness tensor. Thus, the calculated values may not be accurate for the highly boron doped silicon ($N_B \approx 5 \cdot 10^{18}$ 1/cm$^3$) used for the microresonators utilized in this study. Nevertheless, the literature data allows an order-of-magnitude comparison of measured resonator nonlinearities and fundamental material limits.

The critical strain amplitude at the hysteresis due to first- and second-order mechanical nonlinearity corrections can be approximated by

$$S_{C1} = \alpha\sqrt{\frac{1}{Y_1^2 Q}}, \quad S_{C2} = \beta\sqrt{\frac{1}{|Y_2|Q}}, \qquad (7)$$

where $\alpha = \sqrt{16/5\sqrt{3}}$ and $\beta = \sqrt{8/3\sqrt{3}}$ [5]. Equation (7) allows an order-of-magnitude estimation of the hysteresis limit for BAW resonators. Based on the computed values for Young's modulus, we estimate for 2–D plate resonator $S_{C2} \approx 1.3 \cdot 10^{-3}$ and $S_{C3} \approx 1.2 \cdot 10^{-3}$. This estimate shows that both the correction terms can be significant.

## IV. Modeling of Nonlinear Vibrations

To accurately simulate the nonlinear vibrations, the distributed nature of stress and strain has to be included in the model. In our devices the resonator modal shape is to a good approximation sinusoidal and the strain is the highest in the center. A full distributed model would be computationally very demanding and therefore the continuum is approximated with a chain of masses connected with nonlinear springs. As shown in Figure 1, a good approximation is obtained with relatively small number of masses. A four mass system appears to be a good compromise between accuracy and simulation speed and is used in this paper. The relationship between nonlinear Young's modulus and spring constants is

$$k(x) = k_0(1 + k_1 x + k_2 x^2)$$
$$k_0 = \frac{AY_0}{L}, k_1 = \frac{Y_1}{L}, \text{ and } k_2 = \frac{Y_2}{L^2}, \qquad (8)$$

where $x$ is the spring stretching, $A$ is the area, and $L$ is the length. The mass-spring chain model has been implemented as an electrical-equivalent model in RF-simulation program Aplac. In addition to mechanical nonlinearity, the equivalent circuit includes an accurate model of the capacitive coupling [2]. Displacement versus frequency responses to a sinusoidal excitation are simulated using harmonic balance analysis.

## V. Measured Nonlinear Vibrations

To characterize the nonlinear vibrations in single-crystal silicon micromechanical resonators, two bulk acoustic wave (BAW) resonator designs shown in Figure 2 were measured. The devices were fabricated by etching a SOI wafer. Both the 1–D and 2–D BAW resonators show high quality factors exceeding 100 000 and operate at frequency of 11.7 MHz and 13.1 MHZ respectively. Further details of these resonators are provided in references [1] and [8].

The measurements were done using a HP4195A network spectrum analyzer with a JFET preamplifier with low (100 Ω) input impedance to rule out resonator loading by the measurement set-up. Figure 3 shows the measured and simulated transmission amplitudes $|S_{21}|$ for the SOI 2–D BAW device shown in Figure 2. At higher drive levels, the resonator peak becomes sharper and shifts down in frequency. This tilting of the peak to the left is to be expected with the first-order nonlinearity $Y_1$ (positive or negative) and with a negative second-order nonlinearity $Y_2$. A positive second-order nonlinearity would cause shifting of the peak to a higher frequency (spring

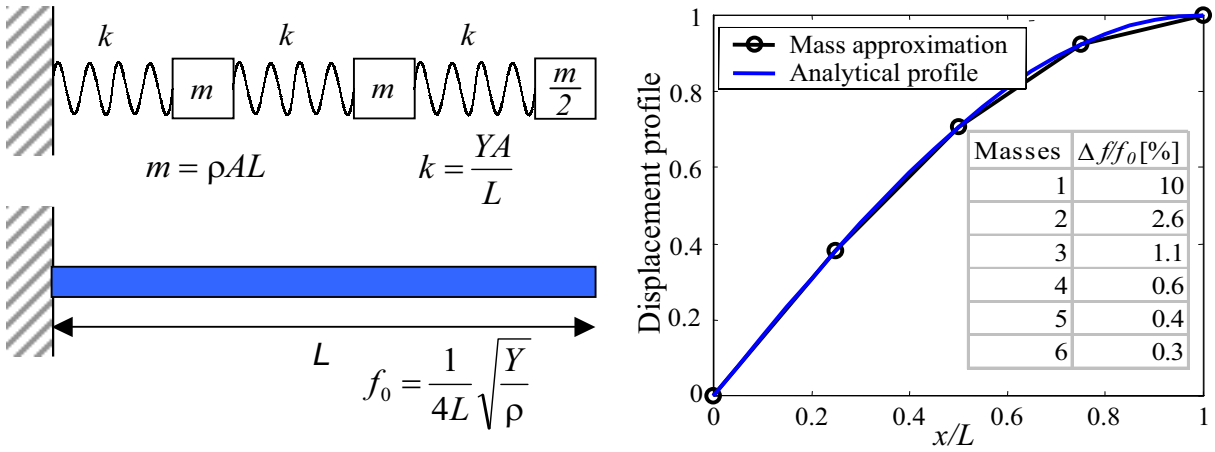


***Figure 1.*** *Equivalent mechanical model used in Aplac circuit simulator. Material nonlinearity is included as nonlinear springs. As the number of discrete elements is increased, the frequency difference $\Delta f / f_0$ between discrete and continuum model approaches zero.*

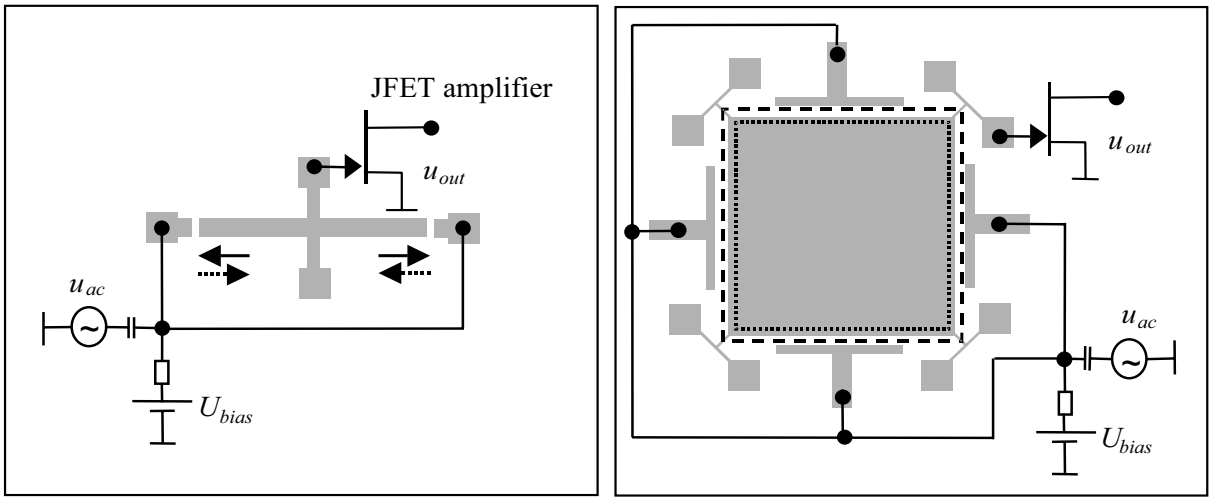


***Figure 2.*** *Schematic of the 1–D and 2–D resonators used in measuring nonlinearities in single-crystal BAW resonators.*

hardening). Increasing the excitation signal causes further increase in nonlinearity and eventually the transmission signal shows discontinuity due to frequency hysteresis.

The measured and simulated data shown in Figure 3(a) correspond to the best fit values $Y_1 = -1.4$ and $Y_1 = -4.0$. These experimentally obtained values are about 50% lower than estimated for a solid plate. This discrepancy can probably be attributed to etch holes in the plate that lower the effective Young's modulus. The maximum vibration amplitude was 220 nm, which corresponds to average strain of $1.4 \cdot 10^{-3}$ and maximum strain of $2 \cdot 10^{-3}$. This corresponds to maximum stored energy of 0.35 $\mu$J or average energy density of $E_m/V = 3.4 \cdot 10^5$ J/m$^3$.

To quantify the effect of nonlinearity due to capacitive coupling, the transmission was also simulated without mechanical nonlinearity in the model. As the capacitive nonlinearity increases as a square of bias voltage, it is insignificant at low bias voltages but becomes important at high bias voltages [1]. This is evident in Figure 3(b), where simulation without mechanical nonlinearity show no excitation amplitude dependence at 50 V bias voltage. Higher bias voltages show capacitive spring softening effect, but even at $U_{bias} = 100$ V this is not enough to explain the observed nonlinearity. A further proof that the mechanical nonlinearity dominates at low bias voltages is obtained by looking at the bias and excitation voltage product $U_{bias} \cdot u_{ac}$ at the hysteresis limit. As the vibration amplitude is proportional to $U_{bias} \cdot u_{ac}$ this remains constant if the mechanical nonlinearity dominates. Our measurements for the 2–D plate clearly show that $U_{bias} \cdot u_{ac}$ is approximately constant indicating that mechanical nonlinearity dominates.

As both the first- and second-order nonlinearity can cause similar distortion on the transmission curve, there is uncertainty about the relative contribution of $Y_1$ and $Y_2$. In principle the nonlinearity could also be characterized by looking at the vibration spectrum. This would allow differentiating between the first- and second-order effects. Unfortunately due to capacitive coupling, even linear vibrations produce harmonics. In our devices, the harmonics due to nonlinear vibrations are below the level of harmonics due to capacitive coupling and thus measuring the current spectrum does not yield informa-

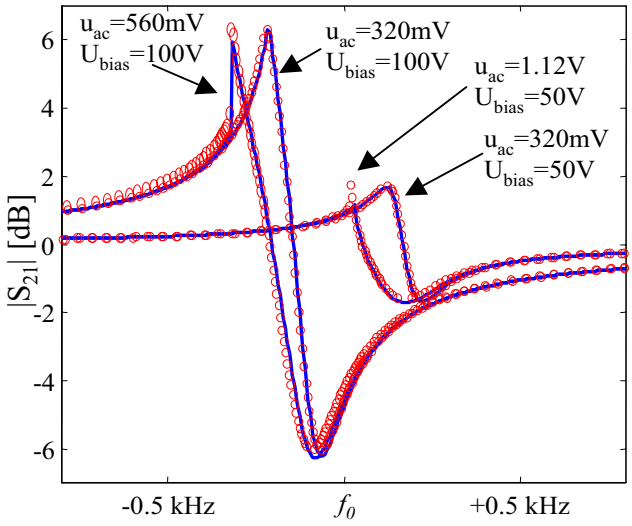


*(a)* Measured (o) and simulated (-) transmission $|S_{21}|$ curves with material nonlinearity included in the model ($Y_1 = -1.4$ and $Y_1 = -4.0$). Highest excitation level results in discontinuity (the sweep shown is from higher to lower frequency).

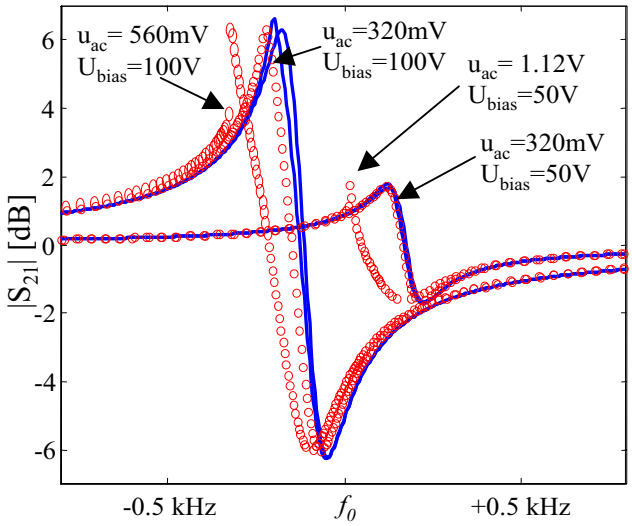


*(b)* Measured (o) and simulated (-) transmission $|S_{21}|$ curves without material nonlinearity included in the model. Capacitive spring softening alone does not explain the frequency shift.

***Figure 3.*** *Measured and simulated transmission curves for 2-D plate ($f_0 = 13.1$ MHz) with nonlinear capacitive and mechanical effects. The maximum vibration amplitude at the hysteresis limit $X_c$ was 220 nm independent of bias showing that hysteresis limit is due to mechanical and not capacitive nonlinearity.*

tion about the mechanical nonlinearity.

The measured 1–D beam BAWs showed similar behavior but the measured values showed larger variation from device to device. This can probably be attributed to the larger surface-to-volume ratio that causes small geometrical or surface defects to have a larger effect. Also, the mechanical spring constant for 1–D beams is much lower than for the 2–D plate causing the capacitive nonlinearity to be comparatively more significant. With capacitive nonlinearity shadowing the mechanical nonlinearity, accurate absolute values for the nonlinear mechanical spring constant could not be obtained. Based on our measurements, we estimate upper limits of $|Y_1| \leq 3$ and $|Y_2| \leq 10$ for the correction terms. Thus, even for the 1-D beam BAWs, we can conclude that the measured mechanical nonlinearities are not significantly larger than estimated from the theory and the devices can be operated near the fundamental strain limit.

The obtained energy density limit $E_m/V = 3.4 \cdot 10^5$ J/m$^3$ for silicon micromechanical resonator can be compared to the hysteresis limit of $E_m/V = 500$ J/m$^3$ for an AT-cut quartz crystal resonator [9]. Thus at least two orders-of-magnitude higher energy density can be achieved with silicon micromechanical resonators than with shear-mode macro quartz devices. This can partially compensate for the small size of RF-MEMS oscillators.

## VI. Conclusions

Nonlinearities in microresonators were identified as the limit for attainable phase noise performance. A model based on a discretization of continuum equations was introduced for the accurate simulation of mechanical nonlinearities. The measured hysteresis strain limit for single-crystal silicon resonators was $2 \cdot 10^{-3}$. This was shown to be close to the fundamental material nonlinearity giving upper of $E_m/V = 3.4 \cdot 10^5$ J/m$^3$ for the energy storage density in silicon microresonator.

## VII. Acknowledgment

We thank A. Alastalo, V. Ermolov, H. Kuisma, and T. Ryhänen for useful discussions. The financial support from Nokia Research Center, VTI Technologies, and Finnish National Technology Agency is acknowledged.

## References

[1] T. Mattila et al., "12 MHz Micromechanical Bulk Acoustic Mode Oscillator", Sensors and Actuators A **101**, 1 (2002).

[2] T. Veijola and T. Mattila, "Modeling of Nonlinear Micromechanical Resonators and Their Simulation with the Harmonic-Balance Method" Int. J. RF and Microwave Computer-Aided Eng. **11**, 310 (2001).

[3] T. Lee, "The Design of CMOS Radio-Frequency Integrated Circuits", (Cambridge University Press, 1998).

[4] G. Sauvage, "Phase Noise in Oscillators: A Mathematical Analysis of Leeson's Model", IEEE Trans. Intrum. and Meas., **26**, 408 (1977).

[5] L. D. Landau and E. M. Lifshitz, Mechanics, 3rd ed., (Butterworth-Heinemann, Oxford, 1999).

[6] K. Y. Kim and W. Sachse, "Nonlinear Elastic Equation of State of Solids Subjected to Uniaxial Homogeneous Loading", J. Material Science **35**, 3197 (2000).

[7] H. McSkimin and P. Andreatch, Jr., "Measurement of Third-Order Moduli of Silicon and Germanium", J. Appl. Phys. **35**, 3312 (1964).

[8] V. Kaajakari et al., "Square-Extensional Mode Single-Crystal Silicon Micromechanical RF-resonator", Transducers'03 (2003).

[9] J. Nosek, "Drive Level Dependence of the Resonant Frequency in BAW Quartz Resonators and His Modeling", IEEE Trans. Ultrasonics, Ferroelectric, Frequency Contr. **46**, 823 (1999).